DOI: 10.1002/ejoc.200700116

Conformation of Trisialic Acid Lactone: NMR Spectroscopic Analysis and Molecular Dynamics Simulation

Chien-Sheng Chen,[a,b] Yi-Ping Yu,[a] Chun-Hua Hsu,[a] Ying-Ta Wu,[c] Wei Zou,[d] Jim-Min Fang,[b,c] and Shih-Hsiung Wu*[a,c]

Dedicated to the memory of Professor Yasuo Inoue

Keywords: Sialic acid / Lactones / NMR spectroscopy / Molecular dynamics / Conformational analysis

The conformation of the trisialic acid lactone α2,8-$(NeuAc)_3$ was analyzed by a combination of NMR spectroscopy, molecular modelling and molecular dynamic (MD) calculations. The interresidue NOEs provided 14 important distance restraints for the molecular simulation, and the final simulated structures showed a root mean square deviation of 0.78 for all superimposed structures. Because of the steric hindrance from the spirobicyclic δ-lactone, the individual sialic acid pyranose rings are considered essential in the chair $_5C^2$ conformation. In addition, lactone I close to the nonreducing end adopted a half-chair $_{A2}HC^{B9}$ conformation, whereas lactone II, which is close to the reducing end adopted a skewed twist-boat $^{C2}S^{C9}$ conformation. In the NMR solution structure and in the 1.0-ns, in-water MD calculation, the final simulated structures are in the exocyclic torsions (ω7, ω8) = (*gauche*–*anti*) surface of the energy adiabatic map, where the global minimum can be found. During the in-water MD simulation, a slight fluctuation in the structure was observed, reflecting the steady conformation of the lactone and the middle residue of the trisaccharide. These data are consistent with a theoretical approach of polysialic acid (PSA) polylactone with torsions (ω7, ω8) = (65°, 175°) and (Φ, Ψ) = (75.8°, –112.4°). Thus, we conclude that the PSA polylactone is a right-hand helix with a rotation angle, μ, of 240° and a repeating unit, n, of 1.5 residues. The structural properties of the PSA lactone discussed within this context differ from the helical epitope of $G2^+$ PSA and may serve in future PSA-related antigen designs.

Introduction

Polysialic acid (PSA) of neural cell adhesion molecules (NCAM), a linear α2,8-linked homopolymer of *N*-acetyl neuraminic acid (NeuAc)[1] and gangliosides with a sialic acid oligomer, play an important role in many biological events.[2] The δ-lactonization in PSA was first observed in 1964.[3] Lifely et al.[4] and Flaherty et al.[5] revealed that the lactonization occurs between the carboxyl group and the 9-hydroxy group from adjacent sialic acid residues, whereas in the GD family, δ-lactones in gangliosides are formed between two adjacent sialic acids,[6] and in the GM family, between the sialic acid and the hydroxy group at the 2- or 4-position of the neighbouring galactosyl residue.[7] Gross et al.[8] provided evidence for a ganglioside lactone in vivo,[9] but failed to isolate it. Gangliosides are involved in regulating negative carboxylate and cationic species, including K^+–Na^+–ATPase,[10] Mg^{2+}–Ca^{2+}[11] and H^+ associated with nerve membrane. However, it is still unclear what role, if any, is played by δ-lactonization in these biological events. The anionic charges in these molecules may be critical to cell recognition and differentiation; thus, lactonization alters the cell surface landscaping and may have significant consequences. In any case, the conformational change associated with lactonization is of interest. Here, we report the first conformational analysis of a trisialic acid lactone by NMR spectroscopy and its molecular dynamic (MD) simulation.

[a] Institute of Biological Chemistry, Academia Sinica, Taipei 115, Taiwan
Fax: +886-2-2653-9142
E-mail: shwu@gate.sinica.edu.tw
[b] Department of Chemistry, National Taiwan University, Taipei 106, Taiwan
[c] Genomics Research Center, Academia Sinica, Taipei 115, Taiwan
[d] Institute for Biological Sciences, National Research Council of Canada, Ottawa, Ontario K1A 0R6, Canada

Supporting information for this article is available on the WWW under http://www.eurjoc.org or from the author.

Results and Discussion

We previously reported studies on the acid/base-catalyzed lactonization/delactonization of α2,8-$(NeuAc)_n$, $n \leq 5$[12] monitored by capillary electrophoresis; regioselective lactonization was observed. In the current study, we obtained the α2,8-$(NeuAc)_3$ lactone from α2,8-$(NeuAc)_3$ by

treatment with glacial acetic acid according to the previously reported procedure. The lyophilized lactone product was analyzed without further purification; therefore, sodium acetate was present as indicated by the proton signal at δ = 1.88 ppm (Figure 1a). δ-Lactonization resulted in a marked downfield shift (1.0–1.5 ppm) of the $^{B}H^{9}$ and $^{C}H^{9}$ protons, and a significant downfield shift (δ =0.8 ppm) of the $^{B}H^{8}$ and $^{C}H^{8}$ protons relative to $^{A}H^{8}$, which appeared at δ_H = 3.26 ppm. Similarly, the $^{B}C^{9}$ and $^{C}C^{9}$ resonances in the ^{13}C NMR spectrum also showed downfield shifts of about 3–5 ppm as a result of lactonization. These diagnostic changes allowed both proton and carbon signals in the HMQC and HMBC spectra to be easily assigned (see Supporting Information). Both the proton and carbon chemical shifts of residue A at the nonreducing end were similar to those in colominic acid,[13] whereas residues B and C at the central site and reducing end, respectively, showed chemical shifts similar to those of colominic acid polylactone.[5]

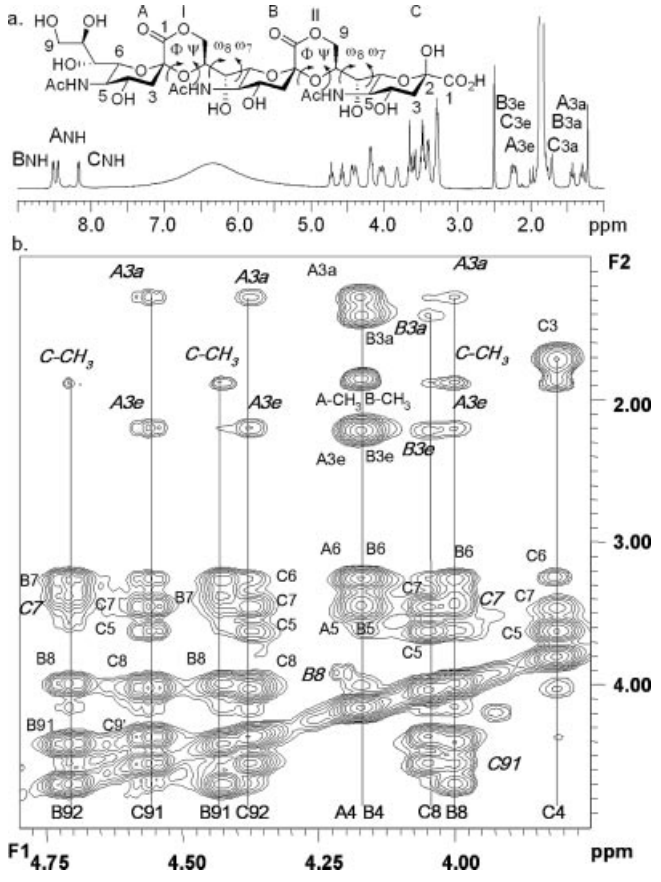

Figure 1. NMR spectrum of α2,8-$(NeuAc)_3$ dilactone in [D_6]-DMSO at 500 MHz: a) Full ^1H NMR spectra. Two exocyclic torsions are ω7 = (O6–C6–C7–O7) and ω8 = (O7–C7–C8–O8), and two glycosidic angles are Φ = (O6–C2–O8–C8) and Ψ = (C2–O8–C8–C7). b) Partial 2D NOESY with a mixing time of 400 ms. The interresidue NOE resonance are shown in italic boldface.

After fully assigning the chemical shifts of all protons, we examined their NOEs and performed molecular simulation. In the partial 2D NOESY spectrum of the α2,8-$(NeuAc)_3$ lactone (Figure 1b), the $^{C}H^{91}$ at 4.567 ppm was distinguished from the $^{C}H^{92}$ at 4.377 ppm on the basis of the occurrence of a medium-range (2.0–4.0 Å) NOE in the $^{B}H^{8}$–$^{C}H^{91}$ pair and the lack of an NOE in the $^{B}H^{8}$–$^{C}H^{92}$ pair. The signals for $^{B}H^{91}$ and $^{B}H^{92}$ were similarly assigned on the basis of their NOE intensities, where $^{B}H^{91}$–$^{C}CH_3$ (NHAc) showed a greater NOE than $^{B}H^{92}$–$^{C}CH_3$. The NOE evidence to determine germinal protons was obtained by analyzing the NOESY spectra with a gradient mixing time to exclude NOE diffusion.

The $_5C^2$ conformation of the individual sialic acid pyranose ring[14] was confirmed by the strong intraresidue (2.0–3.5 Å) NOEs between H^6 and H^4, and between H^5 and H^{3a}. The *trans* diaxial orientation of the $^{A}H^{3a}$–$^{A}H^{4}$ and $^{B}H^{3a}$–$^{B}H^{4}$ pairs was indicated by the large coupling constants (^3J > 10 Hz). Owing to shielding effects, the axial $^{A}H^{3a}$ and $^{B}H^{3a}$ in the interresidue lactones of the α-anomeric configuration occurred at 1.286 and 1.421 ppm, considerably upfield shifted relative to α-sialic acid (1.7–1.5 ppm).[15] In contrast, the sialic acid C at the reducing terminal was in the β-anomeric configuration, in which the equatorial H^{3a} appeared at lower fields (1.9–1.6 ppm) than those in the α configuration, which is in agreement with previous results.[16]

Fourteen interresidue NOEs between three sialic acid residues were observed (Table 1). The NOEs between $^{n}H^{3}$–$^{n+1}H^{8}$ from two adjacent sialic acids ($^{A}H^{3a}$–$^{B}H^{8}$, $^{A}H^{3e}$–$^{B}H^{8}$, $^{B}H^{3a}$–$^{C}H^{8}$ and $^{B}H^{3e}$–$^{C}H^{8}$) indicated δ-lactonization. Some weak NOEs (2.0–5.0 Å) from $^{n}H^{9}$–$^{n+1}H^{CH_3}$ (NHAc) pairs, $^{B}H^{91}$–$^{C}H^{CH_3}$ and $^{B}H^{92}$–$^{C}H^{CH_3}$, were also observed and were similar to those observed in extended poly-α2,8-$(NeuAc)_3$.[13] Notably, $^{B}H^{8}$ contributed eight NOEs by interaction with the neighbouring protons within 5 Å, including the NOE pairs ($^{n}H^{8}$–$^{n+1}H^{91}$, $^{n}H^{8}$–$^{n+1}H^{7}$) of $^{B}H^{8}$–$^{C}H^{91}$ and $^{B}H^{8}$–$^{C}H^{7}$ with medium-range intensities. The long-range NOEs between $^{A}H^{3e}$–$^{C}H^{91}$, $^{A}H^{3a}$–$^{C}H^{91}$, $^{A}H^{3e}$–$^{C}H^{92}$ and $^{A}H^{3a}$–$^{C}H^{92}$ indicated the presence of a turn structure rather than an extended chain.

Table 1. The 14 interresidue NOEs for α2,8-$(NeuAc)_3$ lactone.

Entry[a]	NOE pairs	Range[b]	Entry[a]	NOE pairs	Range[b]
A.	$^{n}H^{3}$–$^{n+1}H^{8}$		C.	$^{n}H^{9}$–$^{n+1}H^{CH_3}$	
1.	$^{A}H^{3a}$–$^{B}H^{8}$	M	9.	$^{B}H^{91}$–$^{C}H^{CH_3}$	W
2.	$^{A}H^{3e}$–$^{B}H^{8}$	M	10.	$^{B}H^{92}$–$^{C}H^{CH_3}$	W
2.	$^{B}H^{3a}$–$^{C}H^{8}$	W	D.	$^{n}H^{8}$–$^{n+1}H^{CH_3}$	
4.	$^{B}H^{3e}$–$^{C}H^{8}$	W	11.	$^{B}H^{8}$–$^{C}H^{CH_3}$	W
B.	$^{n}H^{3}$–$^{n+2}H^{9}$		E.	$^{n}H^{8}$–$^{n+1}H^{91}$	
5.	$^{A}H^{3a}$–$^{C}H^{91}$	M	12.	$^{B}H^{8}$–$^{C}H^{91}$	M
6.	$^{A}H^{3e}$–$^{C}H^{91}$	M	F.	$^{n}H^{8}$–$^{n+1}H^{7}$	
7.	$^{A}H^{3a}$–$^{C}H^{92}$	M	13.	$^{B}H^{8}$–$^{C}H^{7}$	W
8.	$^{A}H^{3e}$–$^{C}H^{92}$	M	G.	$^{n}H^{8}$–$^{n-1}H^{4}$	
			14.	$^{B}H^{8}$–$^{A}H^{4}$	W

[a] Entries A–G are used to classify the 14 interresidue NOEs into sequential groups. [b] The observed intensities were classified into four groups. Very strong (VS), strong (S), medium (M) and weak (W) ranges were assigned distance limits of 1.8, 2.0–3.5, 2.0–4.0 and 2.0–5.0 Å, respectively. Only limits within the W and M ranges were observed for the interresidue ^1H–^1H pair.

With 80 NOE distance restraints and 12 torsional restraints, 100 structures were refined by using the simulated annealing program Xplor NIH.[17] Of these 100 structures, 11 candidates with the lowest energy were selected for further analysis. These structures met the criteria of having a total energy <27 kcal/mol and no NOE violation >0.5 Å for distance restraints. In addition, six angle restraints were used to maintain a $_5C^2$ sialic acid ring conformation, and another six angle restraints were used to keep the NHAc at C^5 in a plane with the amide bond in the *trans* configuration. Although the large coupling constants (>11 Hz) of H^{91} and H^8 indicated the *anti* or eclipsed conformation in $^{C}H^8$–$^{C}H^{91}$ and $^{B}H^8$–$^{B}H^{91}$, the lactone ring conformation was not rigid in the calculations. Therefore, the NOE restraints were the only driving force to affect the conformation of the lactone rings. Superimposing each conformation with the mean conformation yielded average root mean square deviations (RMSD) of 0.78 Å for all conformers (Figure 2), and 0.79, 0.45 and 0.18 Å for residues A, B and C, respectively. The high vibration appeared at the nonreducing residue A because its side chain (C^7–C^8–C^9) was not confined in lactone formation.

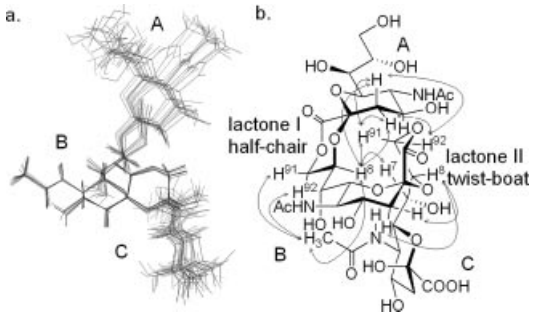

Figure 2. Structures of α2,8-$(NeuAc)_3$ lactone: a) All structures of 11 final sets from simulated annealing calculations with RMSD 0.78 Å were superimposed. b) 2D-Orientation of the conformers in lowest energy. Arrows depict 14 interresidue NOEs pertinent to the turn conformation. The final conformers of lactone rings were indicated as half-chair and skew twist-boat for lactones I and II, respectively.

On the basis of the NOEs and the distance restraints from molecular simulation, lactone I adopted a half-chair $_{A2}HC^{B9}$ conformation, and lactone II adopted a skewed twist-boat $^{C2}S^{C9}$ conformation (Figure 3a). With the C–CO–O of the δ-lactone in the planar form, a slight rotation of the $^{A}C^2$–$^{B}O^8$ and $^{B}O^8$–$^{B}C^8$ bonds in the skew conformation of lactone II would lead to an *S* conformation. We also considered two other possible boat conformers, $^{B2}B^{C9}$ and $_{A2}B_{B9}$ (Figure 3b), as they are often the conformation of δ-lactones in natural products.[18] However, the simulation of $^{B2}B^{C9}$ and $_{A2}B_{B9}$ showed torsional strain in the eclipsed C^8–C^9 bonds and severe hindrance from the 1,2-diaxial, 1,3-diaxial and 1,4-flagpole interactions. In comparison, the half-chair and skewed twist-boat ($_{A2}HC^{B9}$ and $^{C2}S^{C9}$) conformations resulted in less hindrance. Furthermore, the dihedral angle between H^8 and H^{91} is ca. 120° in the $^{B2}B^{C9}$ or $_{A2}B_{B9}$ conformation, which contradicts the observed large coupling constant ($^3J_{8,91}$ > 10.0 Hz); thus, the putative $^{B2}B^{C9}$ and $_{A2}B_{B9}$ boat conformations were excluded. The restrained spirocyclic δ-lactone, as in the α2,8-$(NeuAc)_3$ dilactone, might decrease the optical rotation, and showed negative additivity of the molar ellipticity with respect to oligosialic acid in the circular dichroism spectra.[19] Indeed, α2,8-$(NeuAc)_3$ dilactone exhibited a negative Cotton effect in accordance with the back octant rule (Figure 3c).[20]

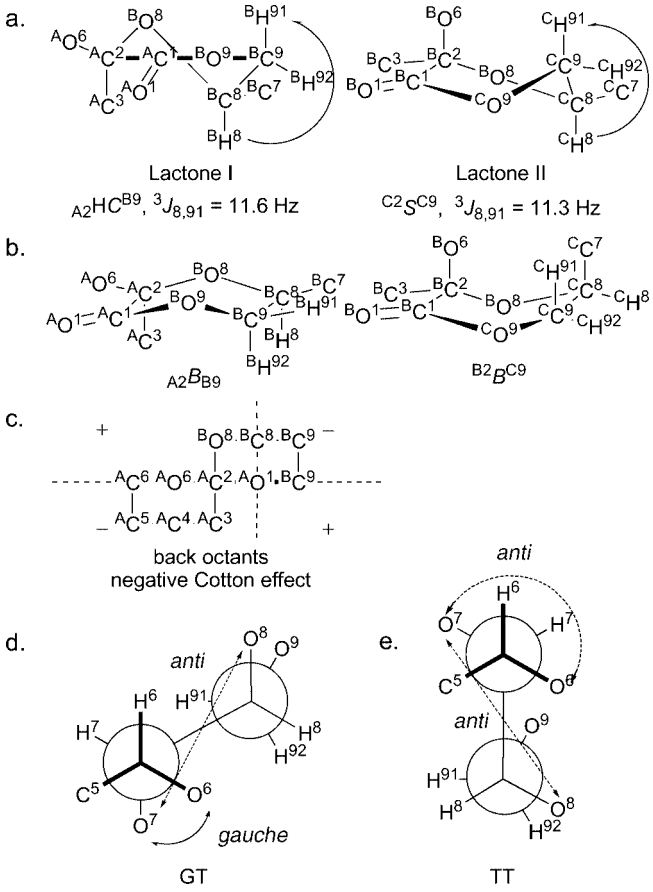

Figure 3. Structural representations of lactones I and II of α2,8-$(NeuAc)_3$ dilactone: a) Lactone I is in the half-chair conformation, and lactone II is in the skewed-boat conformation. The $^3J(^1H,^1H)$ coupling constants for H^8 and H^{91} of individual lactones are indicated. b) Other two possible boat conformers, $_{A2}B_{B9}$ and $^{B2}B^{C9}$, are compared with the $_{A2}HC^{B9}$ and $^{C2}S^{C9}$ conformers. The result indicates that $_{A2}B_{B9}$ and $^{B2}B^{C9}$ likely do not exist owing to severe steric hindrance. c) The pyranose $_5C^2$ connected to δ-lactone as a spirocyclic lactone compiles back octants to give a negative Cotton effect. The (d) *gauche–anti* (GT) and (e) *anti–anti* (TT) conformations of the exocyclic torsional angles ω7 and ω8 is viewed from the Newman projection.

The molecular simulation[21] also provided information on the noncyclic torsions of ω7 = (65 ± 6.3°) and ω8 = (180 ± 8.0°) between residues B and C as the *gauche–anti* (GT) conformers (Figure 3d). The calculated adiabatic conformational energy map, (Figure 4a) illustrated that the exocyclic torsions of the α2,8-$(NeuAc)_3$ lactone were in the 4 kcal/mol well and were in equilibrium. This contour map was obtained by rotation of the noncyclic angles (ω7, ω8) of the α2,8-$(NeuAc)_2$–glycerol lactone, which contains two sialic acids and two lactones. The simulation was initiated by the NMR solution structure with (65°, 180°) as the GT

conformer. The surface of the exocyclic hydroxymethylenyl group C^6–C^7–C^8 was not in diagonal symmetry, which differs from the contours of the glycosidic oxygen of a disaccharide.[22] In comparison, each local minimum in the adiabatic (ω7, ω8) conformational energy map indicated that the α2,8-$(NeuAc)_3$ lactone with less exocyclic torsion is not as floppy as often observed in the carbohydrates with the exocyclic glycosidic linkage C–O–C.[23] The global minimum located at (69°, 176°) was supported by the solution structure determined by NMR spectroscopy. There are five noteworthy minima found within those surfaces in the 10 kcal/mol energy well and within the interresidue NOE distances. Assuming the proton $^{B}H^8$ as the centre of this turn structure, the interresidue NOE pairs ($^{B}H^8$, $^{C}H^7$) between residues B and C were converted into distance contours in adiabatic maps to derive the encompassing minimum centred around (69°, 176°) as allowed by the GT well. A broad minimum centred at (–171°, 161°) is also in agreement with the NOE distance selection, but with 5 kcal/mol higher energy than the global minimum; it was thus considered as the less stable conformation. All the interresidue NOE events (Table 1) were projected on a potential energy surface and examined in accordance with the map. Three encompassed minima (0°, 220°), (54°, 302°) and (–28°, 154°) could be fenced by carrying the torsion (ω7, ω8); nevertheless, those regions outside of the NOE allowance were eliminated.

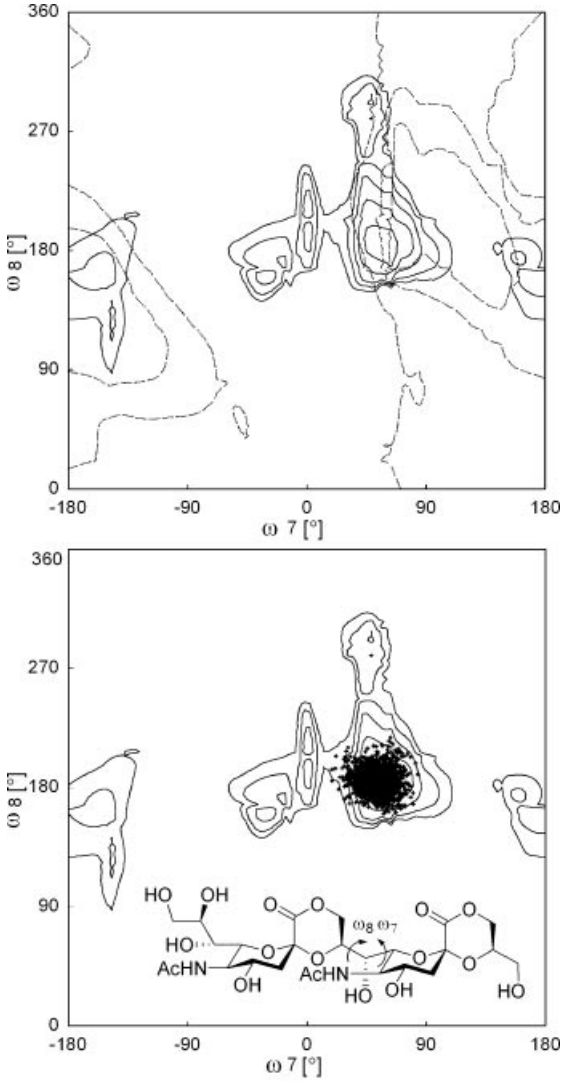

Figure 4. The relaxed adiabatic conformational energy maps (solid line) in the ω7, ω8-space of α2,8-$(NeuAc)_2$ lactone in vacuo, calculated on an 18° × 18° grid and contoured at 2-kcal intervals from 2.0 to 10.0 kcal/mol above the energy minimum. a) Proton ($^{B}H^8$, $^{C}H^7$) distance map (dashed line) of α2,8-$(NeuAc)_3$ dilactone as a function of $^{B}ω7$ and $^{B}ω8$. Contours are in 1-Å intervals from 3.0 to 5.0 Å. b) The 1.0-ns, in-water MD simulation ($^{B}ω7$, $^{B}ω8$) trajectories of the central residue of α2,8-$(NeuAc)_3$ dilactone starting from the NMR solution structure were superimposed.

Because carbohydrate molecules usually occur in an aqueous environment, we carried out a 1.0-ns, in-water MD simulation at 300 K. The NMR solution structure in the GT energy well without the observed NOE distance restraints was deliberately chosen as the starting structure. The internal motions concentrated on the fluctuations of C^6–C^7 and C^7–C^8 across the hydroxymethylenyl linkage. The deviation of fluctuation about the exocyclic torsions across the hydroxymethylenyl carbon was expected to be smaller than the glycosidic torsions (Φ, Ψ) of glycosidic oxygen. The in-water MD (ω7, ω8)-trajectory of the central residue B in the α2,8-$(NeuAc)_3$ lactone was superimposed onto the adiabatic map (Figure 4b). An abecedarian comparison with the average values of torsion statistics (ω7, ω8) between NMR solution and in-water MD are in the same energy surface well. In addition, the mean values of ($^{B}ω7$, $^{B}ω8$) = (65.5°, 172.6°) and ($^{C}ω7$, $^{C}ω8$) = (62.5°, 177.1°) of 1.0-ns, in-water MD also supported this torsional trend. Without NOE distance restraints, the average values of torsion statistics provided the approximate mean values even closer to the initial NMR solution structure. Thus, the in-water MD is an appropriate model for the representation of the α2,8-$(NeuAc)_3$ lactone in water as a dilute solute, and the population of ω7 and ω8 angles in residue C is larger than in residue B. This deduction is mainly due to the central B residue suffering from more steric hindrance than the terminal C residue.

The time series of Φ_A and Φ_B (Figure 5) showed slight fluctuations with mean values 154.4° for Φ_A and 75.8° for Φ_B during the in-water simulation. In comparison with the fluctuation of $^{B}ω7$ and $^{B}ω8$, the glycosidic torsions (Φ, Ψ) appeared to be more strained by the formation of the spirocyclic δ-lactone. An immediate decrease from 135.7° to 101.9° of Φ_A in the range of 215 to 286 ps and a marked increase from 88.6° to 120.2° of Φ_A in the range of 773 to 792 ps were observed. Even in these two periods, the conformations of lactone I and II were only slightly twisted and equilibrated with the relative local minima. It is reasonable to assume that lactone I is still in the *HC* conformer while lactone II is in the *S* conformer throughout the in-water simulation. A considerable interconversion between $_2HC^9$ and $^2S^9$ conformations could proceed by rotating the Φ and ψ angles of the 2,8-sialyl linkages. However, previous studies[24] indicated that the *S* conformer of the δ-lactone is more stable than *HC* by 6.5 kcal/mol, and the conformers

HC and *S* of the α2,8-$(NeuAc)_3$ lactone can be further strained by the spirobicyclic ring in the relative local minima.

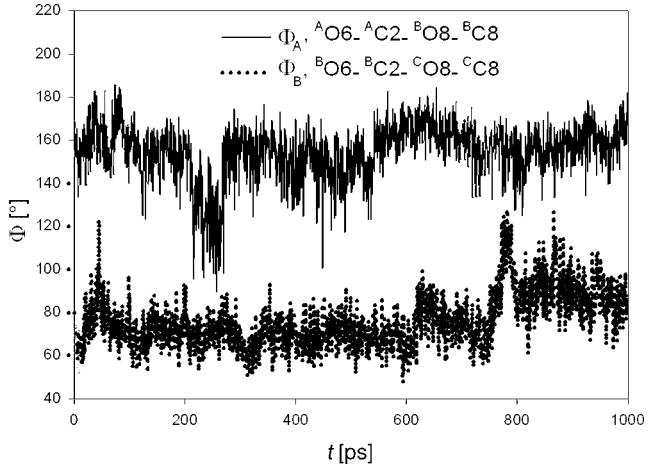

Figure 5. History of Φ_A and Φ_B data collections for the 1.0-ns, in-water MD trajectories.

The NOE distance restraints were recorded in a DMSO ($\varepsilon = 40$) solution. Since carbohydrate molecules usually have identical conformations in water and in DMSO solutions, as supported by the MD simulation of the solvation structure and the behaviour of the carbohydrate molecule in water and in water/DMSO,[25] the NMR spectroscopic study of the carbohydrate molecules in DMSO, which revealed the existence of hydrogen-bonded networks, is comparable to studies of X-ray crystal structure.

Recently, Haselhorst et al.[26] identified the conformation of α2,8-$(NeuAc)_5$ together with endosialidase NF as a helical $G2^+$ structure (Figure 6a), which incorporate the glycerol chain about the C^6–C^7 and C^7–C^8, respectively, in a *gauche–gauche* conformation for ω7–ω8. This is consistent with previous results on the helical epitope of colominic acid, α2,8-$(NeuAc)_n$.[13] On the other hand, Michon et al.[13c] studied the $J_{7,8}$ coupling constants of α2,8-$(NeuAc)_3$ and showed nonexclusive values between the reducing end NeuAc (9.1 Hz) and the nonreducing end saccharide (6.9 Hz), in contrast to the small coupling constant ($J_{7,8} < 3$ Hz) observed in the resolution-enhanced spectrum of colominic acid, as evidence for the *gauche* configuration of the C^7–C^8 bond. The coupling constants may account for the conformations of the glycerol chain about the C^6–C^7 and C^7–C^8, that is, GT in sialic acid and GG in colominic acid. A molecular calculation of α2,8-$(NeuAc)_2$ showed the GT population of C^6–C^7–C^8 as a local minimum and the T2 conformer with helical character ($n = 3$), as described by Brisson et al.[13a] The *anti* configuration of ω8 was eliminated because of the unfavourable electrostatic interactions between the carboxyl groups on adjacent residues. Therefore, the intramolecular lactonization between the carboxylic acid and the hydroxy group would reduce the negative charge density and promote the *anti* conformer of ω8 in the α2,8-$(NeuAc)_3$ lactone.

Residue B, as the central lactone unit of α2,8-$(NeuAc)_3$ dilactone, exhibited slight fluctuations during the NOE-based simulation and the 1.0-ns, in-water MD, and might be relevant to the structure of the middle residue in PSA polylactone. The theoretical studies of the helical epitope in a homogeneous α2,8-sialic acid polysaccharide often suggested data consistent with the NMR spectroscopic experiments. A steady model for decamer nonalactone was established by replicating residue B with exocyclic torsions (ω7, ω8) = (65°, 175°) as the *gauche–anti* conformer and the terminal lactone with the skew twist-boat $^2S^9$ conformation (Figure 6b). The conformation for this PSA lactone shows a right-hand helical chain, and the structure repeats after three residues per turn. Two adjacent residues on each turn show a distance of $h = 4$ Å in the z direction and a rotation angle $\mu = 240°$ in the xy plane. The repeating unit $n = 1.5$ factor is derived from the rotation angle (μ) about the helix axis per repeat unit, following $n = 2\pi/\mu$.[27] All the interresidue NOE pairs listed in Table 1 remarkably coincided with this helical model, with the exception of several interresidue NOEs that were disallowed by considering the lactone in the *HC* conformer. The helical parameters of the PSA lactone are similar to that of the T2 conformer, albeit the glycosidic torsions (Φ, Ψ) = (75.8°, –112.4°) are different from the $G2^+$ conformer.

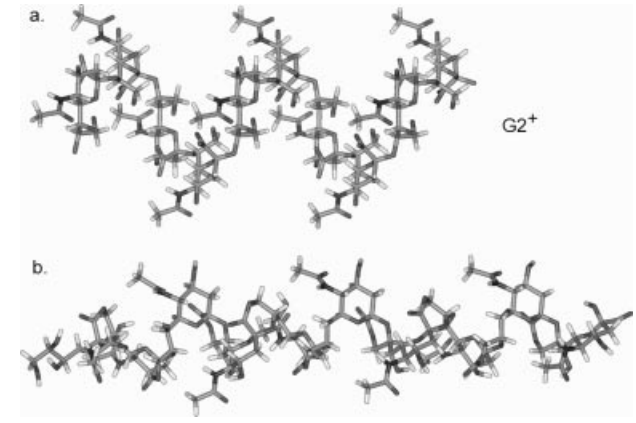

Figure 6. Stereo diagrams of a polysialic acid decamer representing the helical $G2^+$ conformation and the α2,8-$(NeuAc)_{10}$ lactone give integral helices of $n = 4$ (a) and 1.5 (b), respectively.

Conclusions

The natural occurrence of oligosialic and polysialic acid lactones is still not fully understood, and especially esterification in vivo is a conceivable causative factor. We carried out a detailed ^{1}H NMR spectroscopic study of α2,8-linked $(NeuAc)_3$ lactone together with in-water molecular dynamics simulation to demonstrate its steady turn structure with a rigid repeat unit in the middle of the trisaccharide. Furthermore, the theoretical approach indicates that the PSA lactone may exist in a helical conformation having three residues with a pitch of 12 Å, where the lactone ring in the skew twist-boat conformation is located along the helical axis and the exocyclic torsions (ω7, ω8) are in *gauche–anti* conformation. These structural statistics differ

from previous results on the helical epitope of polysialic acid of group B meningococcal polysaccharide. Our results may contribute to a future theoretical and experimental consideration of polysialic acid based antigenic design and hydrolytic resistance against neuraminidase.

Experimental Section

α2,8-(NeuAc)$_3$ Lactone: Tri-*N*-acetylneuraminic acid, α2,8-(NeuAc)$_3$, was obtained from NGK Biochemical Ltd. (Handa, Japan). The α2,8-(NeuAc)$_3$ lactone was synthesized as follows. α2,8-(NeuAc)$_3$ (25 mg, sodium salt) was incubated in glacial acetic acid (4 mL) at room temp. for 48 h, frozen in liquid nitrogen and dried immediately in a SpeedVac (Savant, USA) to remove acetic acid. This freeze-drying procedure was repeated twice. The progress of lactonization was monitored by high-performance capillary electrophoresis (Beckment, P/ACE 2100).

NMR Spectroscopy – Experimental Conditions: NMR spectra were obtained with a Bruker Avance 500 MHz spectrometer in [D$_6$]-DMSO at 300 K, operating at 500.13 MHz for proton and 125.76 MHz for carbon. The sample of α2,8-(NeuAc)$_3$ lactone (8 mg dry wt.) was dissolved in 600 μL [D$_6$]DMSO in a Shigemi NMR tube. Proton and carbon chemical shifts are reported in ppm relative to DMSO at δ_H = 2.49 ppm and δ_C = 39.6 ppm. A set of standard 2D spectra,[30] including COSY, NOESY, HMQC and HMBC experiments, were accumulated in the phase-sensitive mode by using time-proportional phase incrimination (TPPI). The mixing times (τ_m) of the NOESY experiments were 300, 400 and 500 ms. The NOESY data set consisted of 2048 data points in the t_2 dimension and 512 (TPPI method) t_1 increments. In addition, the NMR experiments and NOESY spectra with different mixing times obtained at 300 K were used to differentiate the NOE diffusive effect. The NMR spectroscopic data were processed by using the programs XWIN-NMR 3.1 and Aurelia-Amix 3.1 (Bruker Analytische GmbH).

Restrained Simulated Annealing Calculations: The volumes of NOE cross peaks (400 ms mixing time) were measured. The observed intensities were classified into four groups and compared with the NOE intensity and volume of the cross peak between $^{B}H^{3a}$ and $^{B}H^{3e}$ having a known distance of 1.8 Å. Very strong, strong, medium and weak NOE were assigned to the distance limits of 1.8, 2.0–3.5, 2.0–4.0 and 2.0–5.0 Å, respectively. Three-dimensional structures were generated by using a simulated annealing and energy minimization protocol in the program X-PLOR NIH[17] on a Dell Precision 380 workstation (RedHad Enterprise Linux, WS Version 4). For the construction of the α2,8-(NeuAc)$_3$ lactone, α2,8-(NeuAc)$_3$ was built according to the helix coordination of α2–8-(NeuAc)$_n$ provided by Brisson,[28] and the lactone ring units were further modified using the program INSIGHT II (version 2005.1, Molecular Simulation Inc., San Diego, California, USA). The atom types and topology parameters of the sialic acid residue were compared with previous results on the relevant carbohydrate molecules, and the lactone ring was referred to the PRODRG server.[29] Average structures were calculated by using the final sets of refined structures and further energy was minimized to ensure correct local geometry. INSIGHT II was used to visualize final sets of structures and to draw the electrostatic surface potential of the final 3D models. The convergence of the calculated structures was evaluated in terms of the structural parameters, that is, the RMSD from the experimental distance and dihedral constraints, the values of the energy statistics (*F*noe, *F*tor and *F*repel) and the RMSD from the idealized geometry.

In Vacuum Molecular Statistics: All MDs were performed with a Dell Precision 380 series workstation by using CHARMm (version 31.1) in the INSIGHT II software package. The final ensemble structure of α2,8-(NeuAc)$_3$ dilactone calculated from XPLOR NIH was used as the starting point, and processing passed argument based on topology files of the Quanta package (Accelrys Ins.). The CHARMM force field gave inconsistent primary alcohol sampling (tg > gt > gg) compared to that predicted by experiments (gg > gt > tg); we focused on the relationship between the lactones and the water molecules. The CHARMm force field was used directly owing to the lactonization that reduced the primary alcohol. The force field in XPLOR NIH is also CHARMm, which allowed a reasonable comparison of the MD and NMR conformations. An adiabatic contoured energy surface for α2,8-(NeuAc)$_2$ dilactone was calculated as a function of the exocyclic dihedral angles ω7, ω8 (defined in Figure 1). The related maps were computed by using rigid rotation, followed by harmonic constraint minimization in 10 increments for ω7 and ω8 over the entire angular range; 1369 conformers were generated during each conformational simulation.

MD Simulation Conditions: Cubic periodic boundary conditions were used to simulate a solute to be solvated in a crystal cell. The α2,8-(NeuAc)$_3$ dilactone solution consisted of a box length of 40 Å^3 to obtain 2072 TIP3P water molecules centred about a trisaccharide and an actual concentration 2.29% (w/w, 1.013 g/cm^3). The solution behaviour of α2,8-(NeuAc)$_3$ dilactone was determined by keeping the chemical bonds involving hydrogen atoms fixed through the constraint algorithm SHAKE with 1-fs integration time steps. Interaction between atoms more than 12 Å apart were truncated, and switching functions were used to smoothly turn off long-range interactions between 10 and 11 Å. The solute-containing system was minimized by using a sequence of one steepest-descents minimization within 500 steps (0.01 kcal/mol Å) and one conjugate-gradient minimization within 500 steps (0.01 kcal/mol Å), following heating from the initial temperature of 240 K to a final temperature of 300 K in 80 steps of 10 degrees. The system was equilibrated for a total of 50 ps, followed by production dynamics simulations run for a total of 1000 ps. Equilibration and dynamics were performed by using the velocity Verlet algorithm in steps of 1 fs at a canonical (constant NVT) ensemble of 300 K and 1 atm. Configurations of the molecules were stored at intervals of 0.5 ps in all simulations and analyzed over the entire trajectory.

Supporting Information (see footnote on the first page of this article): HMQC/HMBC assignment, ^{1}H and ^{13}C NMR spectroscopic data, and structural statistics of XPLOR-NIH simulation for α2,8-(NeuAc)$_3$ dilactone.

Acknowledgments

The authors thank Shou-Ling Huang (Instrumentation Center, National Taiwan University), Dr. Shu-Chuan Jao and Prof. Chun-Hung Lin (Institute of Biological Chemistry, Academia Sinica) for helpful discussions. The initial structural coordination of polysialic acid was a gift from Dr. Jean-Robert Brisson (Institute of Biological Science, National Research Council, Canada). This work was supported by the National Science Council and Academia Sinica, Taiwan.

[1] D. Nakata, F. A. Troy II, *J. Biol. Chem.* **2005**, *280*, 38305–38316.

[2] a) Y. Inoue, Y. C. Lee, F. A. Troy II, *Sialobiology and Other Novel Forms of Glycosylation*, Gakushin Publishing, Osaka, **1999**; b) T. Angata, A. Varki, *Chem. Rev.* **2002**, *102*, 439–469;

c) U. Rutishauser, A. Acheson, A. K. Hall, D. M. Mann, J. Sunshine, *Science* **1988**, *240*, 53–57.
[3] E. J. McGuire, S. B. Binkley, *Biochemistry* **1964**, *3*, 247–251.
[4] a) M. R. Lifely, A. S. Gilbert, C. Moreno, *Carbohydr. Res.* **1981**, *94*, 193–203; b) M. R. Lifely, A. S. Gilbert, C. Moreno, *Carbohydr. Res.* **1984**, *134*, 229–243.
[5] T. M. Flaherty, J. Gervay, *Carbohydr. Res.* **1996**, *281*, 173–177.
[6] a) B. Maggio, T. Ariga, R. K. Yu, *Biochemistry* **1990**, *29*, 8729–8734; b) S. Ando, R. K. Yu, J. N. Scarsdale, S. Kusunoki, J. H. Prestegard, *J. Biol. Chem.* **1989**, *264*, 3478–3483; c) G. Fronza, G. Kirschner, D. Acquotti, S. Sonnino, *Carbohydr. Res.* **1989**, *195*, 51–58; d) L. Riboni, S. Sonnino, D. Acquotti, A. Malesci, R. Ghidoni, H. Egge, S. Mingrino, G. Tettamanti, *J. Biol. Chem.* **1986**, *261*, 8514–8519.
[7] a) T. Nakamura, W. A. Bubb, T. Saito, I. Arai, T. Urashima, *Carbohydr. Res.* **2000**, *329*, 471–476; b) T. Terabayashi, T. Ogawa, Y. Kawanishi, *J. Biochem. (Tokyo)* **1990**, *107*, 868–871; c) R. K. Yu, T. A. Koerner, S. Ando, H. C. Yohe, J. H. Prestegard, *J. Biochem. (Tokyo)* **1985**, *98*, 1367–1373.
[8] S. K. Gross, M. A. Williams, R. H. McCluer, *J. Neurochem.* **1980**, *34*, 1351–1361.
[9] a) G. A. Nores, T. Dohi, M. Taniguchi, S. Hakomori, *J. Immunol.* **1987**, *139*, 3171–3176; b) L. Riboni, R. Ghidoni, G. Tettamanti, *J. Neurochem.* **1989**, *52*, 1401–1406.
[10] a) A. Leon, L. Facci, G. Toffano, S. Sonnino, G. Tettamanti, *J. Neurochem.* **1981**, *37*, 350–357; b) Y. Nagata, M. Ando, M. Iwata, A. Hara, T. Taketomi, *J. Neurochem.* **1987**, *49*, 201–207; c) S. E. Karpiak, Y. S. Li, S. P. Mahadik, *Stroke* **1987**, *18*, 184–187.
[11] a) J. P. Behr, J. M. Lehn, *FEBS Lett.* **1973**, *31*, 297–300; b) F. J. Sharom, C. W. Grant, *Biochim. Biophys. Acta* **1978**, *507*, 280–293.
[12] a) M. C. Cheng, S. L. Lin, S. H. Wu, S. Inoue, Y. Inoue, *Anal. Biochem.* **1998**, *260*, 154–159; b) M.-C. Cheng, C.-H. Lin, K.-H. Khoo, S.-H. Wu, *Angew. Chem. Int. Ed.* **1999**, *38*, 686–689; c) M. C. Cheng, C. H. Lin, H. Y. Wang, H. R. Lin, S. H. Wu, *Angew. Chem. Int. Ed.* **2000**, *39*, 772–776; d) Y. P. Yu, M. C. Cheng, H. R. Lin, C. H. Lin, S. H. Wu, *J. Org. Chem.* **2001**, *66*, 5248–5251; e) M. C. Cheng, C. H. Lin, H. J. Lin, Y. P. Yu, S. H. Wu, *Glycobiology* **2004**, *14*, 147–155; f) Y.-P. Yu, M.-C. Cheng, S.-H. Wu, *Electrophoresis* **2006**, *27*, 4487–4499.
[13] a) J.-R. Brisson, H. Baumann, A. Imberty, S. Pérez, H. J. Jennings, *Biochemistry* **1992**, *31*, 4996–5004; b) R. Yamasaki, B. Bacon, *Biochemistry* **1991**, *30*, 851–857; c) F. Michon, J.-R. Brisson, H. J. Jennings, *Biochemistry* **1987**, *26*, 8399–8405; d) A. K. Bhattacharjee, H. J. Jennings, C. P. Kenny, A. Martin, I. C. Smith, *J. Biol. Chem.* **1975**, *250*, 1926–1932.
[14] V. S. R. Rao, P. K. Qasbe, P. V. Balaji, R. Chandrasekaran, *Conformation of Carbohydrate*, Harwood Academic Publishers, Netherlands, **1998**.
[15] R. Schauer, *Sialic acid Chemistry, Metabolism, and Function*, Springer, NY, **1982**.
[16] J. L. Flippen, *Acta Crystallogr. Acta Crystallogr., Sect. B* **1973**, *29*, 1881–1886.
[17] C. D. Schwieters, J. J. Kuszewski, N. Tjandra, G. M. Clore, *J. Magn. Reson.* **2003**, *160*, 65–73.
[18] a) A. M. Mathieson, J. C. Tayler, *Tetrahedron Lett.* **1961**, *2*, 590–592; b) R. C. Sheppard, S. Turner, *Chem. Commun. (London)* **1968**, *9*, 77–78; c) J. F. McConnel, A. M. Mathieson, B. P. Schoenborn, *Tetrahedron Lett.* **1962**, *3*, 445–447; d) H. Wolf, *Tetrahedron Lett.* **1966**, *7*, 5151–5156.
[19] a) T. Terabayashi, M. Tsuda, Y. Kawanishi, *Anal. Biochem.* **1992**, *204*, 15–21; b) T. Terabayashi, T. Ogawa, Y. Kawanishi, *Carbohydr. Polym.* **1996**, *29*, 35–39.
[20] W. Moffitt, R. B. Woodward, A. Moscowitz, W. Klyne, C. Djerassi, *J. Am. Chem. Soc.* **1961**, *83*, 4013–4018.
[21] A. Imberty, S. Perez, *Chem. Rev.* **2000**, *100*, 4567–4588.
[22] a) J. W. Brady, *J. Am. Chem. Soc.* **1989**, *111*, 5155–5165; b) S. B. Engelsen, S. Perez, *J. Mol. Graphics Modell.* **1997**, *15*, 122–131; c) Q. Liu, R. K. Schmidt, B. Teo, P. A. Karplus, J. W. Brady, *J. Am. Chem. Soc.* **1997**, *119*, 7851–7862; d) J. W. Brady, R. K. Schmidt, *J. Phys. Chem.* **1993**, *97*, 958–966.
[23] E. K. Wilson, *Chem. Eng. News* **2004**, *82*, 36–39.
[24] a) B. J. Smith, *J. Phys. Chem. A* **1998**, *102*, 3757–3761; b) K. B. Wiberg, R. F. Waldron, *J. Am. Chem. Soc.* **1991**, *113*, 7697–7705.
[25] A. Vishnyakov, G. Widmalm, J. Kowalewski, A. Laaksonen, *J. Am. Chem. Soc.* **1999**, *121*, 5403–5412.
[26] T. Haselhorst, K. Stummeryer, M. Muhlenhoff, W. Schaper, R. Gerardy-Schahn, M. v. Itzstein, *ChemBioChem* **2006**, *7*, 1875–1877.
[27] H. Sugeta, T. Miyazawa, *Biopolymer* **1967**, *5*, 679–763.
[28] http://www.ibs-isb.nrc-cnrc.gc.ca/facilities/molecularmodelling_e.html.
[29] http://davapc1.bioch.dundee.ac.uk/programs/prodrg/prodrg.html.
[30] S. Braun, H.-O. Kalinowski, S. Berger in *100 and More Basic NMR Experiments*, Wiley-VCH, Weinheim, **1996**.

Received: February 10, 2007
Published Online: June 12, 2007

